Chemical Engineering Journal 171 (2011) 1227–1233

Contents lists available at ScienceDirect

Chemical Engineering Journal

journal homepage: www.elsevier.com/locate/cej

# Kinetics, equilibrium and thermodynamic studies of L-tryptophan adsorption using a cation exchange resin

Youping Xie, Ke-Ju Jing*, Yinghua Lu

*Department of Chemical and Biochemical Engineering, College of Chemistry and Chemical Engineering, Xiamen University, Xiamen 361005, PR China*

ARTICLE INFO

*Article history:*
Received 26 March 2011
Received in revised form 10 May 2011
Accepted 10 May 2011

*Keywords:*
Adsorption
L-Tryptophan
Kinetic
Ion exchange
Equilibrium

ABSTRACT

In this study, the adsorption equilibrium of L-tryptophan by a strong acid styrene cation exchange resin (0 0 1 × 7) was investigated. The equilibrium data were reproduced by both empirical and theoretical treatments. A simple empirical model was able to reproduce the measured total uptake of L-tryptophan. A theoretical model based on ion exchange and the proton transfer reaction was developed to fit the experimental data and to obtain the parameters related to both phenomena. The theoretical model developed herein enables the relation between L-tryptophan uptake, pH and the amount of resin to be determined. Kinetic experiments under different initial L-tryptophan concentrations and initial pHs were performed. The homogeneous particle diffusion model and the shell progressive model were used to define the controlling mechanism of the overall ion exchange process. The results show that the process is always controlled by rate diffusion of L-tryptophan through the polymeric matrix of the resin. The L-tryptophan diffusion coefficient predicted by the homogeneous particle diffusion model in the order of $10^{-9}$ $m^2/s$ is lower than that calculated by the shell progressive model, which has an order of magnitude of $10^{-7}$ $m^2/s$.

## 1. Introduction

L-Tryptophan, one of the essential amino acids widely applied in medicines and animal feeds, is the second least abundant of the common amino acids, generally constituting 1% or less of the average protein mass [1]. Although L-tryptophan has much commercial potential, its application is hampered by high production costs, especially the cost of the downstream processing of the product. In the past, the technology for the production of L-tryptophan was largely based on recovery from protein hydrolysates; today fermentation with genetically engineered bacterial strains constitutes the main production route [2,3]. Several steps are, in general, required in order to recover and purify the L-tryptophan from fermentation broths. Ion exchange is one of the processes that are commonly used for separation of amino acids both on an analytical scale [4] and in industrial manufacturing processes. Since ion-exchange resins exhibit high capacity for amino acids, and the amphoteric nature of amino acids is the advantage for changing the selectivity by adjusting the solution pH [5].

Several attempts were made in the literature in order to systematically study the adsorption equilibrium of amino acids on ion exchange resins and understand how pH, salt concentrations, ionic strength and degree of cross-linking, which play a fundamental role when developing large-scale processes, affect these equilibria [6–12]. However, less research results addressed the basic features of equilibrium and mass transfer characteristics of industrial uses of ion exchange resins for L-tryptophan separations.

In this work, the uptake of L-tryptophan from aqueous solution was evaluated by using a strong cation-exchange resin (0 0 1 × 7). The effect of pH on the extent of ion exchange was studied and several models were used to investigate the interactions of L-tryptophan and the resin as well as the mechanisms which determine the effective uptake.

## 2. Materials and methods

### 2.1. Chemicals

L-Tryptophan (L-Trp, $C_{11}H_{12}N_2O_2$) with purity higher than 98% was supplied by Sigma–Aldrich. Methanol (99.8%, w/w), hydrogen chloride (37%, w/w), sodium dihydrgen phosphate and sodium hydroxide were supplied by Panreac, Spain.

### 2.2. Ion exchange resin

The resin used in this study, 0 0 1 × 7 from Shanghai Resin Factory, China is a commercial sulfonic polystyrene-divinylbenzene

---

* Corresponding author. Tel.: +86 592 2186038; fax: +86 592 2184822.
*E-mail address:* jkj@xmu.edu.cn (K.-J. Jing).

1385-8947/$ – see front matter © 2011 Elsevier B.V. All rights reserved.
doi:10.1016/j.cej.2011.05.031

## Nomenclature

| | |
|---|---|
| $C$ | total concentration of both exchanging species (mol/L) |
| $C_r$ | total concentration of both exchanging species in the ion exchanger (mol/L) |
| $C_0$ | initial concentrations of L-tryptophan in the liquid phase (mol/L) |
| $C^*$ | equilibrium concentrations of L-tryptophan in the liquid phase (mol/L) |
| $C_{S0}$ | concentration of solid reactant at the bead's unreacted core (mol/L) |
| $C_{A0}$ | concentration of species A in bulk solution (mol/L) |
| $D$ | diffusion coefficient in solution phase (cm/s) |
| $D_r$ | diffusion coefficient in solution phase filling the pores resin (cm$^2$/s) |
| $D_{e,r}$ | diffusion coefficient through the reacted layer in the solid phase (cm$^2$/s) |
| $k_s$ | reaction constant based on surface (cm/s) |
| $K$ | equilibrium constant (L/mol) |
| $K_f$ | mass transfer coefficient of species A through the liquid film (cm/s) |
| $K_{IE}$ | ion exchange equilibrium constant |
| $K_{PTR}$ | reaction equilibrium constant (L/mol) |
| $m$ | dissociation parameter |
| $N$ | maximum adsorption capacity (mol/kg dry resin) |
| $q^*$ | equilibrium concentration of L-tryptophan in the resin phase (mol/kg dry resin) |
| $q_{R'SO_3H}$ | total available active sites for ion exchange or proton transfer reaction (mol/kg dry resin) |
| $q^{IE}_{R'SO_3H_3NR}$ | equilibrium concentration of L-tryptophan in the solid phase for ion exchange (mol/kg dry resin) |
| $q^{IE}_{R'SO_3H} = \frac{q^{IE}_{R'SO_3H_3NR}\cdot[H^+]}{q^{IE}_{R'SO_3H}\cdot[^+NH_3{-}R{-}COOH]}$ | available sites of the resin for ion exchange (mol/kg dry resin) |
| $q^{PTR}_{R'SO_3H_3NR}$ | equilibrium concentration of L-Trp in the solid phase for the proton transfer reaction (mol/kg dry resin) |
| $q^{PTR}_{R'SO_3H} = \frac{q^{PTR}_{R'SO_3H_3NR}}{q^{PTR}_{R'SO_3H}\cdot[^+NH_3{-}R{-}COO^-]}$ | available sites of the resin for the proton transfer reaction (mol/kg dry resin) |
| $Q$ | total solid-phase capacity (mol/kg dry resin) |
| $r$ | particle radius (cm) |
| $V$ | initial volume of L-tryptophan solution (L) |
| $W$ | weight of dry ion exchange resin (kg) |
| $X$ | fractional attainment of equilibrium or extent of resin conversion |
| $z$ | stoichiometric coefficient |

strong acid cationic resin. The physical properties of this resin are summarized in Table 1.

The resin was pre-treated by repeated washes with 2 M HCl and 2 M NaOH solutions, and then converted to the hydrogen form by elution with 2 M HCl and rinsed at neutral pH with deionised water.

### 2.3. Analytical method

L-Tryptophan concentration was measured by high-performance liquid chromatography (HPLC). It is applicable to samples with a concentration less than 200 mg/L or samples diluted to fall into this concentration range. An Eclipse XDB-C18, 4.6 mm × 150 mm, 5 μm (Agilent P/N 993967-902) column operating at room temperature and 1 mL/min of mobile phase was used for all measurements. The mobile phase consisted of 85% distilled water with sodium dihydrgen phosphate (0.15%) (Solvent A) and 15% methanol (100%) (Solvent B). The entire run time is 10 min. The detector wavelength (UV) used was 278 nm. Retention time for L-Trp is 6.5 min under these chromatographic conditions. Results obtained were similar and within the range of experimental error.

**Table 1**
Physical and chemical properties of 0 0 1 × 7 resin.

| Type | Strong acidic cation exchanger |
|---|---|
| Standard ionic form | $Na^+$ |
| Functional structure | $-SO_3^-$ |
| Total ion exchange capacity | 1.9 meq/mL or 4.4 meq/g |
| Effective diameter | 0.4–0.6 mm |
| Moisture content | 45–50% |
| DVB cross-linking | 8% |
| Operating pH range | 0–14 |
| Maximum operating temperature | 120 °C |

### 2.4. Equilibrium experiments

Equilibrium isotherms were obtained at various initial pHs and temperatures. The experimental set consisted of twelve 100 mL flasks, hermetically sealed and placed in a constant-temperature shaker bath. The temperature was kept constant within ±0.1 K. For the purpose, 0.5000 g dry resin in hydrogen form was put in contact with 15 mL of solution of known initial L-Trp concentrations. To reach the equilibrium, the suspension formed by the resin and solution was vigorously agitated at 200 rpm for 24 h. Then the mixtures were filtered to remove the ion exchange resin and the filtrate was analyzed for L-Trp content by HPLC, as described above. The resin phase concentration in equilibrium with the liquid phase was obtained by means of the following mass balance equation:

$$q^* = \frac{(C_0 - C^*)V}{W} \tag{1}$$

where $C_0$ and $C^*$ are the initial and equilibrium concentrations of L-Trp in the liquid phase (mol/L), respectively, $q^*$ denotes the resin phase equilibrium concentration of L-Trp (mol/kg dry resin), $V$ and $W$ are the initial volume of L-Trp solution in litres and the weight of dry ion exchange resin in kilograms, respectively.

### 2.5. Kinetic experiments

Kinetics was studied by measuring the rate of L-Trp uptake from the liquid phase by the resin at various initial pHs and concentrations. The experimental set-up consisted of several 100 mL flasks, hermetically sealed and placed in a constant-temperature shaker bath. The temperature was kept at 298 ± 0.1 K. In a typical experiment, 0.5000 g of ion-exchange prewetted resin was placed in contact with 15 mL of L-Trp solution. The mixture was vigorously agitated at 200 rpm for 1000 min and small aliquots of 20 μL were taken out at preset time intervals, and the L-Trp content was analyzed and also, this amount was not considered in the liquid phase for the following steps. On this way, the amount of L-Trp taken out in each sample does not present any effect on the diffusion coefficients obtained.

## 3. Results and discussion

### 3.1. Equilibrium

The type of isotherm has a significant influence on the choice of regeneration conditions [13]. The major parameters affecting the adsorption isotherms were solution pH and temperature in this study.

**Table 2**
Various adsorption isotherm models used to fit the experimental data.

| Model | Equation | Parameters |
|---|---|---|
| Langmuir | $q = \frac{KCN}{1+KC}$ | $K, N$ |
| Freundlich | $q = kC^n$ | $k, n$ |
| Fritz-Schluender | $q = \frac{KNC}{1+NC^m}$ | $K, N, m$ |
| Radke-Prausnitz | $q = \frac{KNC}{(1+KC)^m}$ | $K, N, m$ |
| Tóth | $q = \frac{NC}{(1/K+C^m)^{1/m}}$ | $K, N, m$ |
| Sips | $q = \frac{N(KC)^m}{1+(KC)^m}$ | $K, N, m$ |

**Table 3**
Equilibrium parameters in Eq. (3) of L-Trp on 0 0 1 × 7 resin.

| Parameters | Values |
|---|---|
| $a$ | 0.618 |
| $b$ | −0.0531 |
| $c$ | 0.0041 |
| $K$ (L/mol) | 13.3 |
| $m$ | 0.839 |
| Average deviation (%) $= \frac{\sum_{i=1}^{m} \mathrm{ABS}((q_i^{\exp} - q_i^{\mathrm{theor}})/q_i^{\exp}) \times 100}{m'}$ | 5.14 |

$m'$ = total number of experimental data.

### 3.1.1. Effect of solution pH

For each set of adsorption isotherm data, various adsorption isotherm models [14] listed in Table 2 were tested. The adsorption isotherm models listed in Table 2 can be classified as two-parameter models, such as Langmuir and Freundlich models, and three-parameter models. In general, the three-parameter models fitted the experimental data better than the two-parameter models. Although most models listed in Table 2 except the Freundlich model fitted individual set of data quite well, the associated model parameters varied with the solution pH. Only the Sips model gave best correlations for varying solution pHs. In the Sips model, $N$ represents the maximum adsorption capacity, $K$ the equilibrium constant, and $m$ the dissociation parameter.

The effect of pH on the equilibrium adsorption can be fitted using an empirical equation [15,16]:

$$N = a + bpH + cpH^2 \quad (2)$$

The maximum adsorption capacity may be expected to vary with the solution pH while the equilibrium constant and the dissociation parameter remain unaffected by the solution pH. Introducing Eq. (2) to the Sips equation, the modified Sips model used to predict the adsorption isotherms at varying solution pHs is as follows:

$$q = \frac{(a + bpH + cpH^2)(KC)^m}{1 + (KC)^m} \quad (3)$$

Experimental equilibrium isotherms, together with empirical ones obtained with this model are plotted in Fig. 1. Fitting parameters evaluated by nonlinear least-squares regression analysis and the average deviation between the experimental and empirical data are shown in Table 3. Good agreement between experimental data and model predictions are obtained. However, this empirical model does not allow us to understand the mechanism of ion-exchange process well. To define that process, a theoretical model was developed.

In the liquid phase the L-Trp dissociation takes place according to its $pK_a$ values (2.38 and 9.39). The following dissociation reactions of L-Trp can be proposed in aqueous media as a pH function:

$$[\mathrm{NH_3}^+\text{–R–COOH}] \overset{pK_1=2.38}{\longleftrightarrow} [\mathrm{NH_3}^+\text{–R–COO}^-] + [\mathrm{H}^+] \quad (4)$$

$$[\mathrm{NH_3}^+\text{–R–COO}^-] \overset{pK_2=9.39}{\longleftrightarrow} [\mathrm{NH_2}\text{–R–COO}^-] + [\mathrm{H}^+] \quad (5)$$

where $[\mathrm{NH_3}^+\text{–R–COO}^-]$ is the zwitterionic form of L-Trp, $[\mathrm{NH_3}^+\text{–R–COOH}]$ and $[\mathrm{NH_2}\text{–R–COO}^-]$ are the cationic and anionic form of L-Trp concentrations, respectively.

When the L-Trp content is analyzed, the value measured includes the three forms of L-Trp, i.e.:

$$[\text{L-Trp}_{\text{measured}}] = [\mathrm{NH_3}^+\text{–R–COOH}] + [\mathrm{NH_3}^+\text{–R–COO}^-] + [\mathrm{NH_2}\text{–R–COO}^-] \quad (6)$$

where $[\text{L-Trp}_{\text{measured}}]$ is the total amount of L-Trp in solution with any of the three forms.

The concentrations of the different L-Trp forms in solution as a function of the total concentration of L-Trp and pH of the liquid solution can be obtained by combining the last three equations. The effect of pH on the relative concentrations of three species, with respect to the total concentration of L-Trp in solution is shown in Fig. 2.

The distribution curves show that the anionic L-Trp is present only when pH value is larger than 6. Thus, it would be expected that at the experimental conditions when a strong acid exchanger is involved the zwitterionic and the cationic L-Trp forms would be the main species in solution and the concentration of the anionic form of L-Trp is almost negligible. According to the above comments, it has been assumed that there are two mechanisms for the uptake

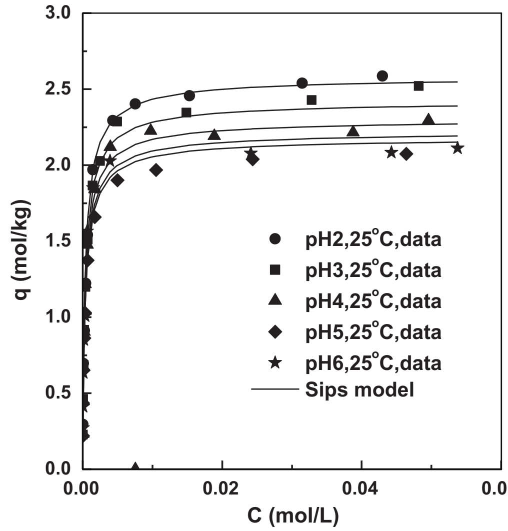

**Fig. 1.** Experimental and Sips-model predicted adsorption isotherms of L-Trp at varying solution pHs.

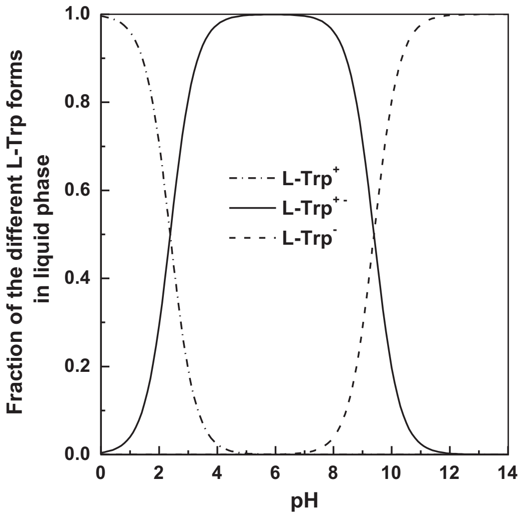

**Fig. 2.** Theoretical concentration distribution of L-Trp species in the liquid phase at 25 °C.

of L-Trp into the resin beads, one by ion exchange and the other by the proton transfer reaction. The cationic form of L-Trp should be loaded into the resin by a conventional ion exchange mechanism:

$$\mathrm{NH_3{}^{+}{-}R{-}COOH + R'{-}SO_3{}^{-}H^{+} \leftrightarrow R'{-}SO_3{}^{-}NH_3{}^{+}{-}R{-}COOH + H^{+}} \tag{7}$$

The zwitterionic form of L-Trp, as we know, can be adsorbed by the hydrogen clays and the strong acid cation-exchange resin in hydrogen form [17], this process may be represented by the proton transfer reaction:

$$\mathrm{NH_3{}^{+}{-}R{-}COO^{-} + R' - SO_3{}^{-}H^{+} \leftrightarrow R'{-}SO_3{}^{-}NH_3{}^{+}{-}R{-}COOH} \tag{8}$$

In this way, $[\mathrm{NH_3{}^{+}{-}R{-}COOH}]$ and $[\mathrm{NH_3{}^{+}{-}R{-}COO^{-}}]$ can be removed by the resin occupying one active centre, releasing one or zero hydrogen ions from the resin active sites, respectively.

If the ideal mass action law is used to represent the above solid–liquid equilibriums, we can obtain:

For ion exchange:

$$K_{\mathrm{IE}} = \frac{q^{\mathrm{IE}}_{\mathrm{R'SO_3H_3NR}} \cdot [\mathrm{H^+}]}{q^{\mathrm{IE}}_{\mathrm{R'SO_3H}} \cdot [\mathrm{NH_3{}^{+}{-}R{-}COOH}]} \tag{9}$$

where $q^{\mathrm{IE}}_{\mathrm{R'SO_3H_3NR}}$ is the equilibrium concentration of L-Trp in the solid phase for ion exchange, $q^{\mathrm{IE}}_{\mathrm{R'SO_3H}}$ the available sites of the resin for ion exchange, $[\mathrm{H^+}]$ the protons concentration in the liquid phase and $K_{\mathrm{IE}}$ the ion exchange equilibrium constant.

On the other hand, for the proton transfer reaction (Eq. (8)):

$$K_{\mathrm{PTR}} = \frac{q^{\mathrm{PTR}}_{\mathrm{R'SO_3H_3NR}}}{q^{\mathrm{PTR}}_{\mathrm{R'SO_3H}} \cdot [\mathrm{NH_3{}^{+}{-}R{-}COO^{-}}]} \tag{10}$$

where $q^{\mathrm{PTR}}_{\mathrm{R'SO_3H_3NR}}$ is the equilibrium concentration of L-Trp in the solid phase for the proton transfer reaction, $q^{\mathrm{PTR}}_{\mathrm{R'SO_3H}}$ the available sites of the resin for the proton transfer reaction and $K_{\mathrm{PTR}}$ the reaction equilibrium constant.

If it is considered that all the active centers could be used indistinctly for ion exchange or the proton transfer reaction, it can be written:

$$q^{\mathrm{IE}}_{\mathrm{R'SO_3H}} = q^{\mathrm{PTR}}_{\mathrm{R'SO_3H}} = q_{\mathrm{R'SO_3H}} \tag{11}$$

According to the above comments, the total capacity of the different resins for L-Trp uptake could be expressed as

$$Q = q^{\mathrm{IE}}_{\mathrm{R'SO_3H_3NR}} + q^{\mathrm{PTR}}_{\mathrm{R'SO_3H_3NR}} + q_{\mathrm{R'SO_3H}} \tag{12}$$

where $Q$ is the total solid-phase capacity, and $q_{\mathrm{R'SO_3H}}$ is the total available active sites for ion exchange or the proton transfer reaction.

Introducing Eqs. (9)–(11) into Eq. (12), leads to:

$$q^{\mathrm{IE}}_{\mathrm{R'SO_3H_3NR}} + q^{\mathrm{PTR}}_{\mathrm{R'SO_3H_3NR}} = Q\,\frac{K_{\mathrm{IE}}[\text{L-Trp}^{+}] + K_{\mathrm{PTR}}[\mathrm{H^+}][\text{L-Trp}^{+-}]}{K_{\mathrm{IE}}[\text{L-Trp}^{+}] + K_{\mathrm{PTR}}[\mathrm{H^+}][\text{L-Trp}^{+-}] + [\mathrm{H^+}]} \tag{13}$$

On the other hand, because the ion exchange occurs between univalent ions, molar units can be used to quantify the process. Thus, the following mass balance can be drawn:

$$q^{\mathrm{IE}}_{\mathrm{R'SO_3H_3NR}} + q^{\mathrm{PTR}}_{\mathrm{R'SO_3H_3NR}} = ([\text{L-Trp}_{\mathrm{initial}}] - [\text{L-Trp}_{\mathrm{measured}}]) \times \frac{V}{W} \tag{14}$$

where $[\text{L-Trp}_{\mathrm{initial}}]$ is the initial L-Trp concentration, $V$ is volume of the solution and $W$ is the weight of dry resin. Eqs. (13) and (14) indicate the global amount of L-Trp removed from the liquid phase.

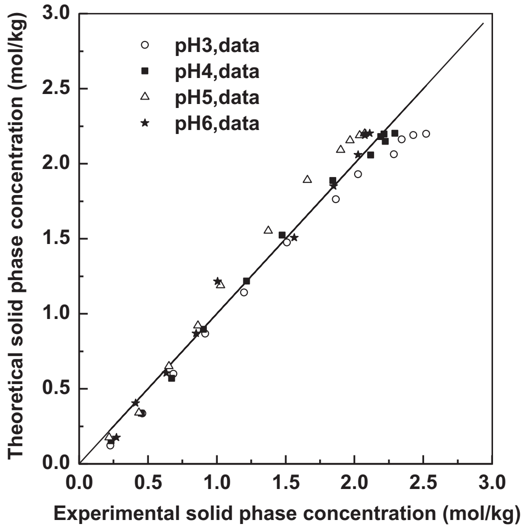

**Fig. 3.** Reproducibility of the experimental data by the theoretical model.

Equaling Eqs. (13) and (14), we obtain:

$$Q\,\frac{K_{\mathrm{IE}}[\text{L-Trp}^{+}] + K_{\mathrm{PTR}}[\mathrm{H^+}][\text{L-Trp}^{+-}]}{K_{\mathrm{IE}}[\text{L-Trp}^{+}] + K_{\mathrm{PTR}}[\mathrm{H^+}][\text{L-Trp}^{+-}] + [\mathrm{H^+}]} = ([\text{L-Trp}_{\mathrm{initial}}] - [\text{L-Trp}_{\mathrm{measured}}]) \times \frac{V}{W} \tag{15}$$

The above equation describes the uptake of L-Trp by the solid in terms of three unknown parameters ($K_{\mathrm{IE}}$, $K_{\mathrm{PTR}}$ and $Q$) related to ion exchange and the proton transfer reaction. Experimental data were fitted to Eq. (15) by a nonlinear least-squares regression procedure (Fig. 3). The values of the parameters obtained by fitting the experimental data to this model are given in Table 4. The results indicate that the value of $K_{\mathrm{IE}}$ is much more than $K_{\mathrm{PTR}}$. It is found that the proton transfer reaction is the predominant process to uptake L-Trp onto 0 0 1 × 7 resin near the isoelectric pH of L-Trp, whereas both ion exchange and the proton transfer reaction are important at lower pH.

### 3.1.2. *Effect of temperature*

The Gibbs free energy change of the ion-exchange process is related to the equilibrium constant with the following equation:

$$\Delta G = -RT \ln K \tag{16}$$

The Gibbs free energy change can be calculated from the entropy change and heat of adsorption at constant temperature by the following equation:

$$\Delta G = \Delta H - T\Delta S \tag{17}$$

Combining Eqs. (16) and (17) leads to

$$K = \exp\left(\frac{\Delta S}{R} - \frac{\Delta H}{RT}\right) \tag{18}$$

**Table 4**
Equilibrium parameters in Eq. (15) of L-Trp on 0 0 1 × 7 resin.

| Parameters | Values |
|---|---|
| $Q$ (mol/kg) | 2.21 |
| $K_{\mathrm{IE}}$ | 14.05 |
| $K_{\mathrm{PTR}}$ (L/mol) | 4.11 |
| Average deviation (%) $= \frac{\sum_{i=1}^{m} \mathrm{ABS}((q_i^{\exp} - q_i^{\mathrm{theor}})/q_i^{\exp}) \times 100}{m'}$ | 9.84 |

$m'$ = total number of experimental data.

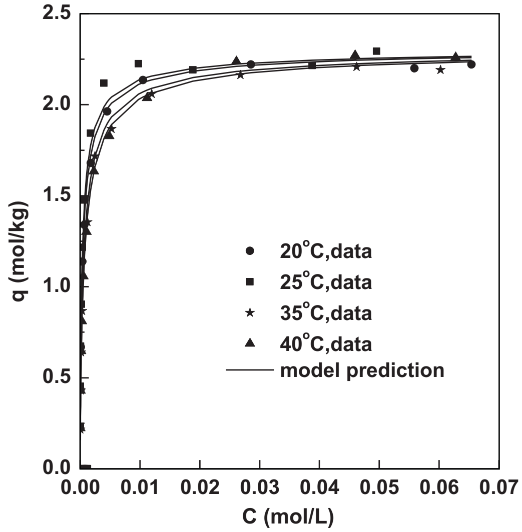

**Fig. 4.** Experimental and Sips-model predicted adsorption isotherms of L-Trp at varying temperatures.

The maximum adsorption capacity and dissociation constant are not affected by the solution temperature while the equilibrium constant depends on the temperature.

Introducing Eq. (18) to the Sips equation, the modified Sips model used to predict the adsorption isotherms at various temperatures is as follows:

$$q = \frac{N(e^{(\Delta S/R)-(\Delta H/RT)}C)^m}{1+(e^{(\Delta S/R)-(\Delta H/RT)}C)^m} \tag{19}$$

Fig. 4 shows the experimental and the predicted adsorption isotherms by modified Sips model at various solution temperatures. The values of the parameters obtained by fitting the experimental data to this model are presented in Table 5.

## 3.2. Kinetics

Ion exchange process could be explained by a number of sequential processes determining the rate of reaction, which include diffusion of solute through the liquid film surrounding the particle (liquid film diffusion control (LFDC)), diffusion of solute through the polymeric matrix of the resin (particle diffusion control (PDC)) and chemical reaction (CR). One of the steps which offers much greater resistance than the others can be considered as the rate-limiting step of the process [18]. The evolution of the L-Trp uptake $q$ (mg L-Trp/g resin) with time at various initial concentrations and pHs are shown in Figs. 5 and 6, respectively. In order to understand the ion exchange kinetic process from the microscopic point of view and to define which mechanism controls the L-Trp uptake, the kinetic models selected to describe the ion exchange data are two models widely used for fitting: homogeneous particle diffusion model (HPDM) and shell progressive model (SPM) [19,20].

**Table 5**
Equilibrium parameters in Eq. (19) of L-Trp on 0 0 1 × 7 resin.

| Parameters | Values |
|---|---|
| $N$ (mol/kg) | 2.31 |
| $\Delta S$ (J/(mol K)) | −68.9 |
| $\Delta H$ (kJ/mol) | −26.6 |
| $m$ | 0.756 |
| Average deviation (%) = $\frac{\sum_{i=1}^{m} \mathrm{ABS}((q_i^{\exp}-q_i^{\mathrm{theor}})/q_i^{\exp})\times 100}{m'}$ | 5.35 |

$m'$ = total number of experimental data.

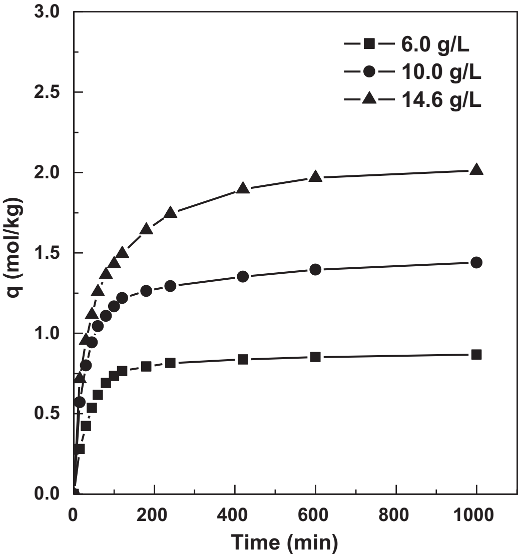

**Fig. 5.** Uptake of L-Trp at different initial concentrations.

### 3.2.1. Homogeneous particle diffusion model

In this model, the ion exchange mechanism involves diffusion of L-Trp ions from the aqueous solution and H$^+$ ions from the resin phase through a number of possible resistances. The species originally in the solution phase must diffuse across the liquid film surrounding the resin particle, transfer across the solution/particle interface, and diffuse into the bulk of the resin particle. The exchange of L-Trp$^+$/H$^+$ can be rigorously described by the Nernst Plank equation. This applies to counter diffusion of two species in a quasi-homogeneous media. Resin phase controlled diffusion of ions from an infinite volume of solution into a spherical ion-exchange particle can be described by the following equation [19–21]:

$$-\ln(1-X^2(t)) = 2Bt \qquad \text{with } B = \frac{\pi^2 D_r}{r^2}, \quad X(t) = \frac{q_t}{q_e} \tag{20}$$

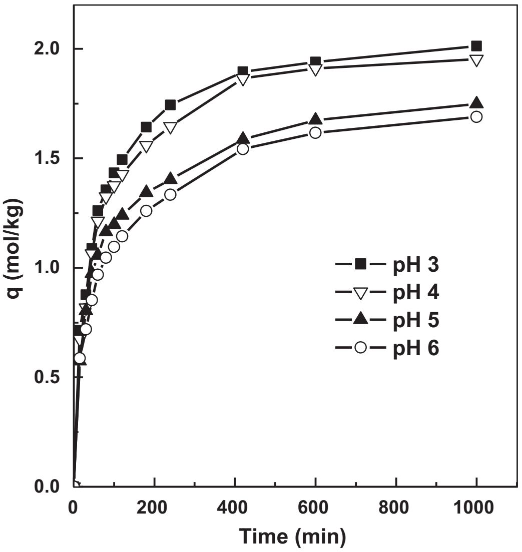

**Fig. 6.** Uptake of L-Trp at different initial pHs.

**Table 6**
Linear regression analysis of HPDM and SPM models for L-Trp uptake at different initial concentrations and pHs onto 0 0 1 × 7 resin.

| | HPDM | | | | | SPM | | | | |
|---|---|---|---|---|---|---|---|---|---|---|
| | $-\ln(1-X^2)$ | | $-\ln(1-X)$ | | $X$ | | $[3-3(1-X)^{2/3}-2X]$ | | $[1-(1-X)^{1/3}]$ | |
| | $R^2$ | $D_r$ (cm²/s) | $R^2$ | $D$ (cm/s) | $R^2$ | $K_f$ (cm/s) | $R^2$ | $D_{e,r}$ (cm²/s) | $R^2$ | $k_s$ (cm/s) |
| *pH* | | | | | | | | | | |
| 3 | 0.99 | $3.95\times10^{-9}$ | 0.94 | $1.87\times10^{-6}$ | 0.83 | $3.28\times10^{-5}$ | 0.99 | $1.31\times10^{-7}$ | 0.91 | $2.35\times10^{-5}$ |
| 4 | 0.98 | $3.90\times10^{-9}$ | 0.94 | $1.80\times10^{-6}$ | 0.83 | $3.26\times10^{-5}$ | 0.98 | $1.30\times10^{-7}$ | 0.91 | $2.33\times10^{-5}$ |
| 5 | 0.98 | $3.73\times10^{-9}$ | 0.91 | $1.57\times10^{-6}$ | 0.80 | $3.22\times10^{-5}$ | 0.97 | $1.24\times10^{-7}$ | 0.88 | $2.28\times10^{-5}$ |
| 6 | 0.98 | $3.15\times10^{-9}$ | 0.90 | $1.37\times10^{-6}$ | 0.79 | $3.02\times10^{-5}$ | 0.98 | $1.06\times10^{-7}$ | 0.87 | $2.08\times10^{-5}$ |
| *Concentration* | | | | | | | | | | |
| 6.0 g/L | 0.99 | $6.43\times10^{-9}$ | 0.99 | $1.90\times10^{-6}$ | 0.88 | $9.25\times10^{-5}$ | 0.99 | $4.98\times10^{-7}$ | 0.97 | $7.35\times10^{-5}$ |
| 10.0 g/L | 0.99 | $6.01\times10^{-9}$ | 0.94 | $1.95\times10^{-6}$ | 0.79 | $5.55\times10^{-5}$ | 0.98 | $2.83\times10^{-7}$ | 0.90 | $4.32\times10^{-5}$ |
| 14.6 g/L | 0.99 | $4.00\times10^{-9}$ | 0.93 | $1.89\times10^{-6}$ | 0.80 | $3.31\times10^{-5}$ | 0.99 | $1.33\times10^{-7}$ | 0.89 | $2.37\times10^{-5}$ |

If liquid film diffusion controls the rate of exchange, the following analogous expression can be used:

$$-\ln(1-X(t)) = K_{li}t \qquad \text{with} \quad K_{li} = \frac{3DC}{rC_r}, \quad X(t) = \frac{q_t}{q_e} \tag{21}$$

### 3.2.2. Shell progressive model

When the porosity of the polymer is small and thus practically impervious to the fluid reaction, the reaction may be explained by the shell progressive approach [22]. The kinetic concept of a shell progressive mechanism can be described in terms of the concentration profile of a liquid reactant containing a counterion A advancing into a spherical bead of a partially substituted ion-exchanger. As the reaction progresses in the bead, the material balance of counterion A follows Fick's diffusion equation with spherical coordinates. In this case, the relationship between reaction time and degree of ion fractional conversion is given by the following expressions [19,23,24].

(a) When the fluid film controls:

$$X = \frac{3C_{A0}K_F}{zrC_{S0}}t \tag{22}$$

(b) When the diffusion though the ion exchange layer controls:

$$[3-3(1-X)^{2/3}-2X] = \frac{6D_eC_{A0}}{zr^2C_{S0}}t \tag{23}$$

(c) When the chemical reaction controls:

$$[1-(1-X)^{1/3}] = \frac{k_sC_{A0}}{r}t \tag{24}$$

The aim of this kinetic study was to find the diffusion model, which better describes the experimental data, and to determine the rate-controlling steps and the kinetic parameters of the mass transfer of L-Trp. Kinetic experimental data were fitted to Eqs. (20) and (21) for the HPDM and Eqs. (22)–(24) for the SPM. The results of the linear regression analysis for the two models are summarized in Table 6. The linear correlations coefficients indicate that particle diffusion can be considered as the rate-limiting step of the process since the fit gives a relatively straight line. Both the homogeneous particle diffusion and the shell progressive models seemed to fit the data well. The slope values were used to calculate effective diffusion coefficients for the different conditions using Eqs. (20) and (23). These calculated diffusion coefficients are in fact a measure of the mean interdiffusion coefficient of the L-Trp involved in the ion exchange process. The mean interdiffusion coefficients given by the homogeneous particle diffusion decrease slightly with increasing initial L-Trp concentration or initial pH. On the other hand, the diffusion coefficients calculated by the shell progressive model decrease with increasing initial L-Trp concentration or initial pH. The decrease with respect to initial concentration is more important in the case of $D_{e,r}$ and this may be due to the accumulation of the product of the reaction in the reaction layer, which hinders the progress of the L-Trp ions within this layer. The comparison of these coefficient shows that the shell progressive model gives higher coefficient values than homogeneous model. This result can be proved by the presence of chemical reaction between the L-Trp ions and the functional structure of resin.

## 4. Conclusions

In order to determine the equilibrium of L-Trp on 0 0 1 × 7 resin, the uptake of L-Trp was reproduced by both empirical and theoretical treatments. Based on the Sips model, an empirical model was able to reproduce the experimental data at different pHs. A theoretical model based on ion exchange and the proton transfer reaction was developed to fit the experimental data and to obtain the parameters related to both phenomena. The theoretical treatment allowed us to verify that the adsorption capacity does not depend on pH. The proton transfer reaction is the predominant process for uptake of L-Trp on 0 0 1 × 7 resin near the isoelectric pH of L-Trp, whereas both ion exchange and the proton transfer reaction are important at lower pH.

In terms of the kinetic experiments, homogeneous particle diffusion and shell progressive models converge to affirm that the rate determination step is the diffusion of L-Trp through the polymeric matrix of the resin. The calculated kinetic parameters show that the interdiffusion coefficients in the reaction layer ($D_{e,r}$) are more important than the diffusion coefficient in the solid phase ($D_r$).

## Acknowledgements

Authors are grateful to the financial support of the Fundamental Research Funds for the Central Universities (2010121049) from China.

## References

[1] R.L. Somerville, Tryptophan: biosynthesis, regulation and large-scale production, in: K.M. Herrmann, R.L. Somerville (Eds.), Amino Acids: Biosynthesis and Genetic Regulation, Addison-Wesley, 1983, pp. 351–378.

[2] S. Azuma, H. Tsunekawa, M. Okabe, R. Okamoto, S. Aiba, Hyper-production of L-tryptophan via fermentation with crystallization, Appl. Microbiol. Biotechnol. 39 (1993) 471–476.

[3] M. Ikeda, R. Katsumata, Hyperproduction of tryptophan by *Corynebacterium glutamicum* with the modified pentose phosphate pathway, Appl. Environ. Microbiol. 65 (1999) 2497–2502.

[4] S. Blackburn, in: G. Zweig, J. Sherma (Eds.), Amino Acids and Amines, CRC Press Inc., Boca Raton, FL, 1983.

[5] S. Takac, G. Calik, M. Aytar, T.H. Ozdamar, Separation kinetics of L-phenylalanine by ion-exchange process, Biochem. Eng. J. 2 (1998) 101–112.

[6] N.H.L. Wang, Q. Yu, S.U. Kim, Cation exchange equilibria of amino acids, React. Funct. Polym. 11 (1989) 261–277.

[7] F.G. Helfferich, Ion-exchange equilibria of amino acids on strong-acid resins: theory, React. Funct. Polym. 12 (1990) 95–100.

[8] S.R. Dye, J.P. Decarli, G. Carta, Equilibrium sorption of amino acids by a cation-exchange resin, Ind. Eng. Chem. Res. 29 (1990) 849–857.

[9] I.L. Jones, G. Carta, Ion exchange of amino acids and dipeptides on cation resins with varying degree of cross-linking. 1. Equilibrium, Ind. Eng. Chem. Res. 32 (1993) 107–117.

[10] S. Melis, J. Markos, G. Cao, Ion-exchange equilibria of amino acids on a strong acid resin, Ind. Eng. Chem. Res. 35 (1996) 1912–1920.

[11] A. Zammouri, S. Chanel, L. Muhr, G. Grevillot, Ion-exchange equilibria of amino acids on strong anionic resins, Ind. Eng. Chem. Res. 39 (2000) 1397–1408.

[12] M.J. Moreira, L.M. Ferreira, Kinetic studies for sorption of amino acids using a strong anion-exchange resin effect of ionic strength, J. Chromatogr. A. 1092 (2005) 101–106.

[13] J.M. Chern, C.Y. Wu, Desorption of dye from activated carbon reds: effects of temperature, pH, and alcohol, Water Res. 35 (2001) 4159–4165.

[14] M.D. LeVan, G. Carta, C.M. Yon, Adsorption and ion exchange, in: Perry's Chemical Engineers, Handbook, seventh ed., New York, 1997.

[15] J.L. Valverde, A.D. Lucas, M. Carmona, M. Gonzalez, J.F. Rodriguez, Equilibrium data of the exchange of $Cu^{2+}$, $Cd^{2+}$ and $Zn^{2+}$ ions for $H^+$ on the cationic exchanger Lewatit TP-207, J. Chem. Technol. Biotechnol. 79 (2004) 1371–1375.

[16] M. Carmona, A.D. Lucas, J.L. Valverde, B. Velasco, J.F. Rodriguez, Combined adsorption and ion exchange equilibrium of phenol on Amberlite IRA-420, Chem. Eng. J. 117 (2005) 155–160.

[17] Z.Y. Tao, H. Zhang, B.L. Zhang, Thermodynamic functions for ion exchange of amino acid, React. Funct. Polym. 27 (1995) 29–33.

[18] M. Ahmaruzzaman, D.K. Sharma, Adsorption of phenols from wastewater, J. Colloid Interface Sci. 287 (2005) 14–24.

[19] L. Liberti, R. Passino, in: J.A. Marinsky, Y. Marcus (Eds.), Ion Exchange Solvent Exchange, vol. 7, Dekker, New York, 1977.

[20] F. Helfferich, Ion Exchange, third ed., McGraw-Hill, New York, 1962.

[21] M. Caetano, C. Valderrama, A. Farran, J.L. Cortina, Phenol removal from aqueous solution by adsorption and ion exchange mechanisms onto polymeric resins, J. Colloid Interface Sci. 338 (2009) 402–409.

[22] J.L. Cortina, R.A. Yellin, N. Miralles, A.M. Sastre, A. Warshawsky, Kinetics studies on heavy metal ions extraction by Amberlite XAD2 impregnated resins containing a bifunctional organophosphorous extractant, React. Funct. Polym. 38 (1998) 269–278.

[23] G. Schmuckler, S. Golstein, in: J.A. Marinsky, Y. Marcus (Eds.), Ion Exchange Solvent Exchange, vol. 7, Dekker, New York, 1977.

[24] M. Benamor, Z. Bouariche, T. Belaid, M.T. Draa, Kinetic studies on cadmium ions by Amberlite XAD7 impregnated resins containing di (2-ethylhexyl) phosphoric acid as extractant, Sep. Purif. Technol. 59 (2008) 74–84.